EPJ AP

Applied Physics

EPJ.org
your physics journal

Eur. Phys. J. Appl. Phys. (2012) 58: 20101 DOI: 10.1051/epjap/2012110311

Polycrystalline silicon thin films on glass deposited from chlorosilane at intermediate temperatures

A.G. Benvenuto, R.H. Buitrago, and J.A. Schmidt

The title “The European Physical Journal” is a joint property
of EDP Sciences, Società Italiana di Fisica (SIF) and Springer

Eur. Phys. J. Appl. Phys. (2012) 58: 20101
DOI: 10.1051/epjap/2012110311

THE EUROPEAN PHYSICAL JOURNAL
APPLIED PHYSICS

Regular Article

Polycrystalline silicon thin films on glass deposited from chlorosilane at intermediate temperatures

A.G. Benvenuto[1], R.H. Buitrago[1,2], and J.A. Schmidt[1,2,a]

[1] Instituto de Desarrollo Tecnológico para la Industria Química (INTEC), CONICET-UNL, Güemes 3450, S3000GLN Santa Fe, Argentina
[2] Facultad de Ingeniería Química, UNL, Santiago del Estero 2829, S3000AOM Santa Fe, Argentina

Received: 5 August 2011 / Received in final form: 29 March 2012 / Accepted: 30 March 2012
Published online: 9 May 2012 – © EDP Sciences 2012

Abstract. We show that commercial float glass can be used as a substrate to deposit polycrystalline silicon (poly-Si) by chemical vapor deposition from trichlorosilane at temperatures between 740 and 870 °C. By using scanning electron microscopy an average grain size lower than 0.4 μm was observed, with a columnar structure suitable for the electrical conduction in photovoltaic cells. X-ray diffraction reveals a strong (2 2 0) preferential orientation of the films, which is indicative of a low density of intra-grain defects. Atomic force microscope images reveal a conical structure, with a root mean square roughness of ∼65 nm for samples of around 3 μm in thickness. This natural texture is a positive characteristic from the point of view of light trapping. By using boron tribromide as a doping agent, degrees of doping ranging from intrinsic to clearly *p*-doped were obtained, as shown by dark conductivity measurements as a function of temperature. The process, the reactants and the substrate used are of low cost and proved to be adequate for direct poly-Si deposition.

1 Introduction

Thin-film polycrystalline silicon (poly-Si) solar cells deposited on low-cost substrates are promising candidates to achieve the expected reduction in the cost of photovoltaic electricity. For that purpose, a careful choice of the deposition process, the reactants and the substrate is essential. Atmospheric pressure thermal chemical vapor deposition (AP-CVD) allows high deposition rates starting from low-cost precursors. It also provides high uniformity, controllable doping profiles and good film quality with a relatively simple setup [1]. The drawback is the utilization of high temperatures, thus increasing the energy consumption to produce the films and imposing restrictions to the materials that can be used as substrate [2]. Despite this, AP-CVD is considered one of the most promising methods to produce thin poly-Si films at low cost.

The most suitable gas precursor – from the point of view of cost – is trichlorosilane (TCS, $SiHCl_3$), which is an intermediate product in the industrial silicon production. $SiHCl_3$ can be obtained by hydrochlorination of metallurgical grade silicon and can be easily purified by distillation. AP-CVD from $SiHCl_3$ has been used by some groups to deposit poly-Si in the range of 1000–1200 °C. Different substrates have been tested, including low-cost silicon [3], metals [4], ceramics [5] and graphite [6]. Some authors have also used high-temperature-resistant glass-ceramic substrates [7]. In reference [8] it is reported that direct deposition from $SiHCl_3$ at 1000 °C was applied to produce solar cells on high-temperature glass substrates, and it is theoretically shown that efficiencies of around 10% could be attained. Corning Inc. developed a glass-ceramic with a strain point above 900 °C (Corning Code 9664) [9], which was used as a substrate for thin-film poly-Si solar cells [10]. The main drawback of these high-temperature glass-ceramics is that they are not floatable, what increases the production costs. Furthermore, in some cases they are not completely transparent to the portion of the solar spectrum usable by a silicon solar cell [9] which would mean a reduction in its efficiency if they were used to produce cells in a superstrate configuration. In addition to the direct deposition of poly-Si on a substrate, another approach is to epitaxially thicken a seed layer. Deposition onto a seeded flat 1-mm-thick glass resulted in an average grain size of 1.6–2.2 μm and a hole mobility of 68 $cm^2\ V^{-1}\ s^{-1}$ [11]. Solar cells with conversion efficiencies of around 2% have been produced by this method [12]. In reference [13], AP-CVD was used to thicken an aluminum-induced-crystallized seed layer. The deposition temperature was 1130 °C, leading to a growth rate of around 1.4 μm/min. The solar cells made by this method achieved a maximum efficiency of 8.0%. Recently, monocrystalline-silicon seed layers were prepared on transparent glass-ceramic substrates by using a patented process that

[a] e-mail: jschmidt@intec.unl.edu.ar

consists of anodic bonding and an implant-induced separation. These layers were then epitaxially thickened by thermal CVD, obtaining simple solar cell structures with efficiencies of up to 7.5% [14]. In all cases, the deposition temperature was higher than 1000 °C, thus excluding the possibility to use float glass as substrate.

In addition to withstanding the process temperature, the substrate's thermal expansion coefficient should match that of crystalline silicon [2]. Moreover, it would be desirable for it to be an insulator that can be produced in the form of large sheets, to allow a monolithic interconnection scheme, and to be transparent, to deposit the cells in a superstrate configuration [10]. Those requirements are fulfilled by an aluminosilicate float glass, such as the AF37 of Schott GmbH, which has a thermal expansion coefficient of 3.77×10^{-6} K^{-1} and a softening point of 942 °C [15]. To use this glass as a substrate for the deposition of poly-Si, it remains to be tested if AP-CVD can produce films of acceptable quality at temperatures lower than 900 °C. It is well known that the grain size of poly-Si deposited by AP-CVD decreases when the deposition temperature is decreased [16]. However, it has also been shown that solar cells produced from poly-Si having a grain size lower than 0.2 μm can lead to open-circuit voltages larger than 530 mV [17].

In this work, we demonstrate that a simple deposition process (AP-CVD), a cheap precursor ($SiHCl_3$) and a low-cost substrate (commercial aluminosilicate glass) can be combined to produce poly-Si thin films of good structural and electrical characteristics. Working in an intermediate temperature range between 740 and 870 °C we achieve acceptable deposition rates, and we obtain films exhibiting high crystallinity and columnar structure suitable for the vertical conduction in photovoltaic devices. A strong preferential (2 2 0) orientation is also indicative of a low density of intra-grain defects. Therefore, we suggest a possible new route to produce low-cost polycrystalline silicon solar cells.

2 Experimental procedures

The CVD reactor that we use is a batch-type, hot-wall reactor, consisting of a horizontal quartz tube located inside a tubular oven. The reaction takes place inside the quartz tube. This configuration presents the advantage of producing a preheating of the reaction gases before they reach the substrates, which are located between 15 and 23 cm from the oven inlet, in a region of nearly uniform temperature. The preheating of the reaction gases proved essential for the reaction to take place. Hot-wall reactors show high electrical power utilization efficiency, provided that a resistance-heated furnace with good thermal insulation is used.

Sheets of Schott AF37 glass, 0.3 cm thick × 0.8 cm wide × 2.5 cm long, were used as substrates. The precursor compound was trichlorosilane, and hydrogen was used as carrier and reaction gas. A constant flow of 38 sccm of hydrogen was made to bubble in the liquid precursor, whose temperature was kept at 0 °C. The vapor pressure of TCS at 0 °C is about 209 Torr, and since the process was carried out at atmospheric pressure, the partial pressure of hydrogen was approximately 551 Torr. Consequently, the proportion of the precursor in the gas mixture was about 27%. All the samples presented in the present study are intrinsic except otherwise stated.

A series of runs was carried out using three substrates in each experiment. The substrates were placed one behind the other, and their location in the quartz tube (between 15 and 23 cm from the oven inlet), as well as the precursor temperature (0 °C), hydrogen flow (38 sccm) and experiment time (30 min) were kept constant for all the runs. For each run the oven temperature was set 20 °C higher than in the previous one, starting from 760 °C and up to 880 °C, which gave rise to substrate temperatures (T_s) from 740 °C to 870 °C, approximately. The whole series of experiments was carried out twice in order to verify the repeatability of the results. The samples were structurally characterized by optical microscopy, scanning electron microscopy (SEM), atomic force microscopy (AFM), X-ray diffraction and reflectance spectroscopy in the UV-Vis region. Evaporated Al electrodes were deposited on top of the samples for electrical contacts, disposed in a coplanar geometry with a separation of 1 mm between them. The ohmicity of the contacts was verified. Dark conductivity was measured as a function of temperature between 170 and 25 °C, placing the samples inside a cryostat evacuated to a base pressure of $\sim 10^{-6}$ Torr. Hall effect measurements were performed in the van der Pauw configuration, applying a magnetic field of 0.65 T.

3 Results and discussion

The global chemical reaction leading to silicon deposition can be written as:

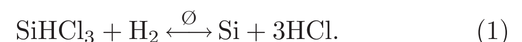

$$SiHCl_3 + H_2 \xleftrightarrow{\varnothing} Si + 3HCl. \qquad (1)$$

Trichlorosilane reduces at high temperature in the presence of hydrogen, resulting in the deposition of silicon and the release of hydrochloric acid. The reaction is reversible, meaning that under certain conditions silicon can be etched by HCl [4]. The reaction efficiency depends on the reactant concentrations, temperature and pressure. For the conditions that we use, the films become dense and uniform, with a good coverage and adhesion to the substrate.

The thickness of the poly-Si films was calculated through the interference peaks of the reflectance spectrum in the range of 400–900 nm. The deposition rate was calculated dividing the thickness by the deposition time (30 min in all cases), assuming that the incubation period is short compared to the total deposition time. The dependence of the deposition rate on the deposition temperature, for a constant location of the substrates in the reactor, is presented in Figure 1. It is a well-known result that the deposition of poly-Si by CVD exhibits a transition temperature between two growing regimes: the reaction-rate-limited regime and the mass-transport-limited regime.

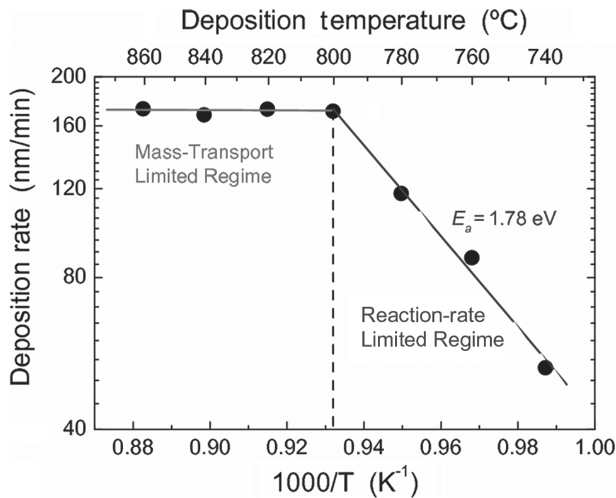

Fig. 1. (Color online) Deposition rate of poly-Si films on glass substrates versus temperature for a 27% initial concentration of TCS in the gas mixture.

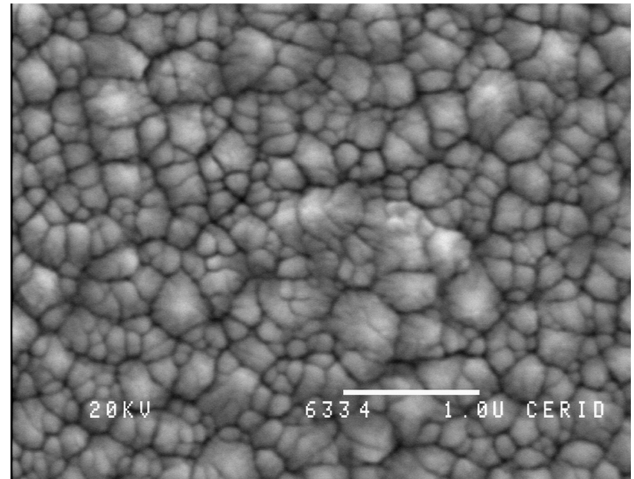

Fig. 2. *SEM* image of a film deposited at 792 °C. The bar has a length of 1 μm.

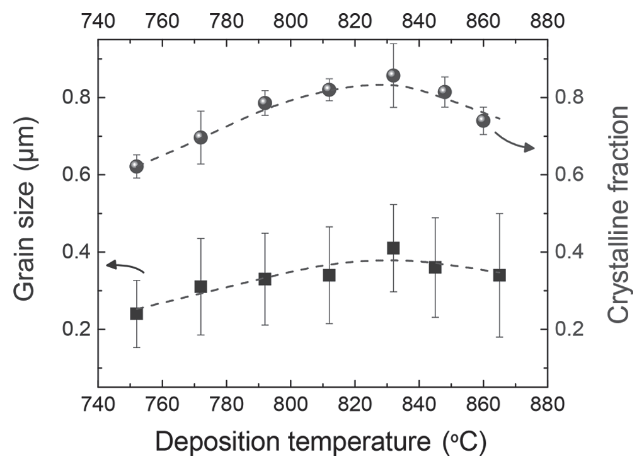

Fig. 3. (Color online) Grain size and crystalline fraction as a function of deposition temperature. The lines are guides to the eye.

For the glass substrates and the deposition parameters of this work, the transition temperature is 800 °C. Using graphite substrates, a TCS/H_2 ratio of 15%, boron doping and a total gas flow rate of 3.3 slm in a rapid thermal CVD reactor, Angermeier et al. [18] found that the transition between both regimes occurs at 1000 °C. The substrate and the design of the reactor play a key role in defining the transition between both deposition regimes. In our experiment, below 800 °C the deposition rate is limited by the surface reaction kinetics, which is thermally activated with an activation energy of ~1.78 eV. The deposition rate increases exponentially with temperature in this range. Above 800 °C, on the other hand, the rate-limiting factor is the mass delivery of the species toward the surface. In this mass-transfer-controlled regime, all the silicon-producing species reaching the substrate contribute to silicon deposition. Therefore, for the deposition conditions that we use, a temperature-independent deposition rate of ~170 nm/min is obtained in this mass-transfer-controlled regime.

Scanning electron microscopy was used to explore the front surface and the cross-section of the samples. The grain size and the structure were evaluated from these images. Figure 2 presents a picture of the surface of a sample deposited at 792 °C, without any surface treatment. A compact structure can be seen, with a relatively high dispersion in the grain size. The average grain size is in this case (0.33 ± 0.12) μm.

The average grain size, evaluated from an analysis of the SEM images, is presented in Figure 3 as a function of the deposition temperature (squares). As can be seen, the grain size increases slightly with the deposition temperature, from ~250 nm for T_S = 750 °C to ~370 nm for T_S = 865 °C. The general tendency of the grain size to increase with the deposition temperature is in agreement with the results from other authors, who found a similar dependence [16] although in a different temperature range. The dispersion in grain size within one film is also a frequent characteristic of the deposition of poly-Si by CVD [18,19]. On the other hand, the grain size obtained by other authors is usually in the range of 1–10 μm, much larger than what we have obtained here. This is probably due to the higher temperatures used in those works, usually between 1100 and 1200 °C, which can be applied to substrates like silicon, graphite or ceramics [16–19]. However, the non-transparent substrates make the production of the cells in the superstrate configuration impossible. Moreover, the use of float glass substrates would be a great advantage in terms of cost reduction. For the glass substrates that we use we are limited to operate under 880 °C, and the maximum grain size that we obtain is 0.41 μm for T_S = 832 °C. Nevertheless, open-circuit voltages around 540 mV have been demonstrated even for fine-grained poly-Si (average grain size ~0.2 μm) [17]. The grain size that we obtain should not be a limitation for the obtainment of good photovoltaic properties, provided that the intra-grain quality is acceptable and the grain boundaries are of low electronic activity.

The UV reflectance spectra of the samples can be used to estimate the crystalline fraction (X_C) of the poly-Si films. The UV reflectance spectrum of crystalline silicon is characterized by two prominent peaks, located at ∼280 and ∼365 nm, corresponding to the optical interband transitions at the X point and along the $\Gamma - L$ axis of the Brillouin zone, respectively [20]. Crystalline fraction is usually evaluated by the quotient [21]

$$X_C = \frac{R_1 - R_2}{R_1^{c-\text{Si}} - R_2^{c-\text{Si}}}, \quad (2)$$

where R_1 and R_2 are the measured reflectances at $\lambda \approx 280$ and 365 nm, respectively, and the superscript "c-Si" refers to the known values of single crystalline silicon. According to reference [21], the definition of X_C is based on the fact that the 280 nm peak intensity is influenced by crystallinity and also by surface roughness while the 365 nm one accounts mainly for roughness. Figure 3 (circles) presents the dependence of the crystalline fraction on the deposition temperature. As can be seen, in the reaction-rate-limited regime there is an almost linear increase of X_C with deposition temperature. A maximum value of $X_C \approx 85\%$ is obtained for $T_S = 832\,°\text{C}$, in accordance with the maximum grain size. Finally, there is a slight decrease of both grain size and X_C for the highest deposition temperatures. The close agreement between both parameters is due to the fact that a lower grain size implies a larger volume proportion of grain boundaries, which are defective regions of reduced crystallinity. A crystalline fraction of ∼85% is consistent with a grain size in the range of 400 nm.

Figure 4 presents the results of AFM observations of a sample deposited at 772 °C, which is typical for the whole series of samples. A conical structure can be observed, with grain dimensions that are compatible with the SEM observations. The root mean square (RMS) roughness, evaluated from the AFM observations, is 65 nm for this 3-μm-thick sample. The surface roughness can be described as natural texturing of the surface, and it is considered a positive characteristic for its contribution to light trapping. A thin-film Si solar cell requires highly efficient light-trapping designs to absorb a significant fraction of the incident sunlight. The morphology of these layers would allow increasing the optical path length of light within the solar cell structure. The texture that we observe may be a result of the chemical etching of the growing silicon film, due to the presence of HCl at elevated temperatures. This compound, which is a by-product of the chemical reaction of silicon deposition, has been used in some works to control the process of silicon nucleation due to its etching activity [1,22].

Figure 5 shows a SEM image of the cross-section of a sample deposited at 860 °C. The structure of all the films of the series is predominantly columnar, what makes them suitable for the vertical electrical conduction in devices like solar cells, since the transport of charge carriers does not involve crossing grain boundaries. A similar columnar structure has been found in poly-Si thin films deposited

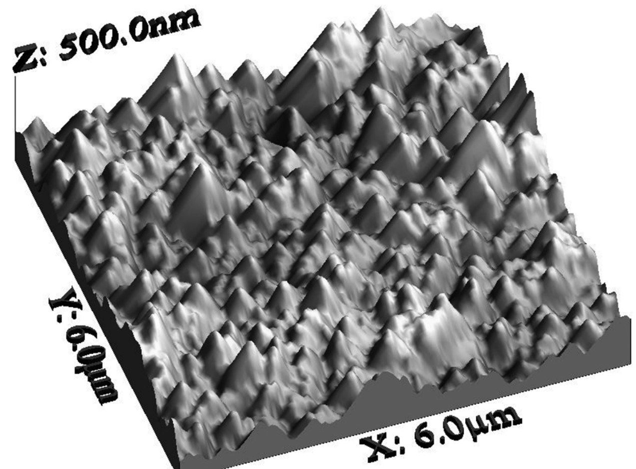

Fig. 4. (Color online) AFM image of a sample deposited at 772 °C. The dimensions of the three axes are shown in the figure.

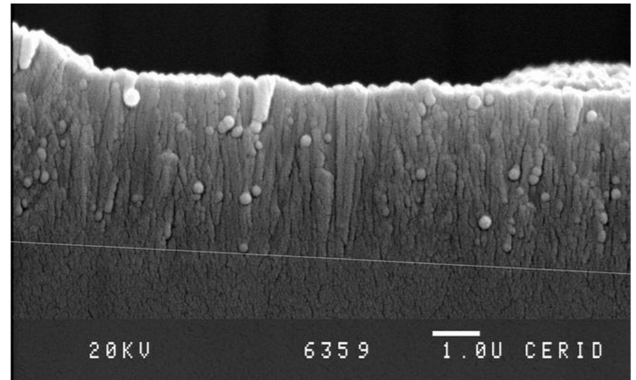

Fig. 5. SEM image of the cross-section of a thin poly-Si film deposited at 860 °C. The length of the bar is 1 μm. The line indicates the interface between the glass and the poly-Si film.

at higher temperatures on different substrates, as shown in references [16–19,23,24].

X-ray diffraction was used to evaluate the crystalline orientation of the poly-Si films. For all the deposition temperatures that we used, we have found a clear preferential orientation with the (2 2 0) plane parallel to the sample surface. Figure 6 shows the X-ray diffraction spectrum of a film deposited at about 830 °C. A high intensity peak can be seen for 2θ equal to 47.3°, corresponding to the (2 2 0) plane, and much lower peaks at 28.4° and 56.1°, corresponding to the (1 1 1) and (3 1 1) planes, respectively. This is evidence of a preferential (2 2 0) orientation.

To quantify the degree of preferential orientation of the films, we have calculated the orientation factor α_{hkl}, defined by the formula [24]:

$$\alpha_{hkl} = \frac{I_{hkl}/I_{0,\,hkl}}{\sum_{hkl} I_{hkl}/I_{0,\,hkl}} \times 100, \quad (3)$$

where I_{hkl} is the measured intensity for the $(h\ k\ l)$ plane and $I_{0,hkl}$ is the intensity of the corresponding Si

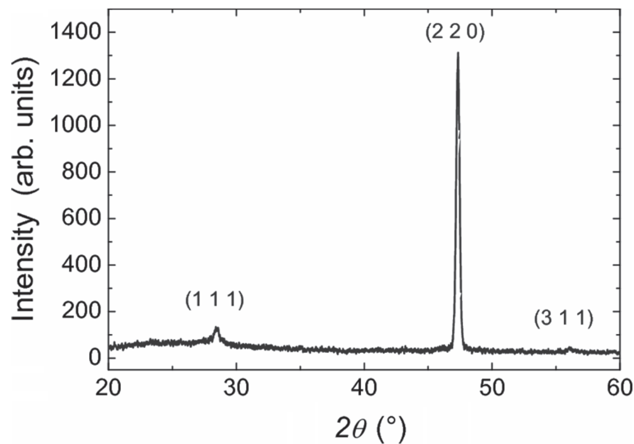

Fig. 6. (Color online) X-ray diffraction spectrum of a poly-Si film deposited at ∼830 °C. A preferential (2 2 0) orientation can be seen.

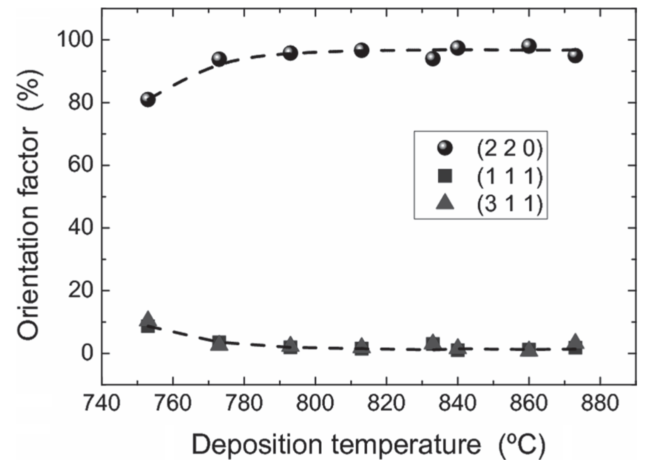

Fig. 7. (Color online) Orientation factor α as a function of the deposition temperature for the series of samples studied. The lines are just guides to the eye.

powder diffraction peak used as a standard reference. This factor, which quantifies the volume fraction of grains with the specified orientation, is presented in Figure 7 as a function of deposition temperature. The X-ray diffraction measurements exhibit a strong (2 2 0) preferential orientation, close to 95% for samples deposited in the mass-transport-limited regime. The (1 1 1) and (3 1 1) orientations only present some significant contribution for the lowest temperatures. At lower deposition temperatures, in the reaction-rate-limited regime, the surface atoms are able to migrate to stable sites, favoring the lateral growth of different crystallographic planes. The precursor gases do not react immediately due to kinetics limitations, and the accumulation of adsorbed atoms to shape a growing front has a better chance of increasing by capturing species in the diffusion layer. The preferential (2 2 0) orientation of the columnar-grained layers is considered a favorable characteristic. The growth of poly-Si with a preferential (2 2 0) orientation on different substrates is also mentioned in several publications [16,19,24], although a degree of orientation as high as the one obtained here has only been obtained utilizing dichlorosilane [25], a less used and more expensive silicon precursor. This orientation is usually associated with the growth of columnar grains and with a low recombination activity at the grain boundaries. The (2 2 0) texture ensures that many grain boundaries should be of the [1 1 0]-tilt type. Such grain boundaries are electrically inactive and they grow without broken bonds [26]. The columnar structure shown in Figure 5 and the preferential (2 2 0) orientation shown in Figure 7 are both favorable characteristics for photovoltaic applications.

The electrical characterization of the samples involved measurements of dark conductivity as a function of temperature, thermopower and Hall effect. For all the samples in the series, an activated behavior of the dark conductivity has been found. Figure 8 (circles) presents an Arrhenius plot of dark conductivity as a function of inverse temperature for an intrinsic sample deposited at ∼830 °C. The activation energy results in this case $E_a = 0.535$ eV

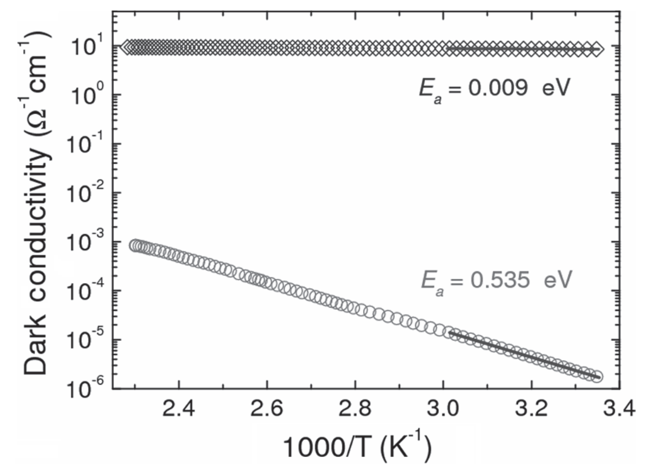

Fig. 8. (Color online) Dark conductivity as a function of inverse temperature for an intrinsic sample deposited at $T_S \approx 830$ °C (circles) and for a boron-doped sample deposited at $T_S \approx 850$ °C (diamonds). The activation energies obtained from linear fits in the low temperature regions are indicated in the figure.

and the room-temperature dark conductivity is $\sigma_{\mathrm{dk}}(25\ °\mathrm{C}) = 1.7 \times 10^{-6}\ \Omega^{-1}\ \mathrm{cm}^{-1}$. Both E_a and $\sigma_{\mathrm{dk}}(25\ °\mathrm{C})$ reveal the intrinsic nature of this sample. For the whole series of samples, the activation energy values are in the range of 0.45–0.54 eV, without a definite tendency as a function of deposition temperature. The activation energies measured for this series of samples are an indication of the absence of substantial contamination in the deposition system that we use. Thermopower measurements also revealed that electrons are the majority carriers in these undoped samples.

In order to demonstrate the possibility to produce p-doped poly-Si films, we have introduced in our reactor controlled amounts of tribromoborine (BBr_3) as a boron source. The partial pressure of BBr_3 was controlled by adjusting its temperature between −35 and +30 °C, and therefore the proportion of dopant in the samples was varied. Figure 8 also presents (diamonds) the dark

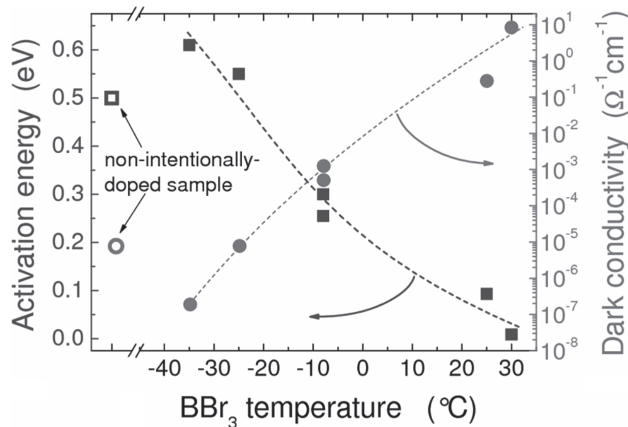

Fig. 9. (Color online) Room-temperature dark conductivity (circles, right scale) and activation energy (squares, left scale) as a function of BBr_3 temperature. The first points to the left correspond to the nominally intrinsic sample. The lines are guides to the eye.

conductivity as a function of inverse temperature for a doped sample deposited at a substrate temperature of $\sim$850 °C and a BBr_3 temperature of +30 °C. The room-temperature dark conductivity of $\sim$8 Ω^{-1} cm^{-1} and the activation energy of $\sim$0.009 eV indicate that doping is effective, thus demonstrating the possibility of depositing *p*-doped layers by using the same low-cost deposition method.

Figure 9 (circles, right scale) shows the room temperature dark conductivity of a series of doped samples, as a function of the BBr_3 temperature (proportional to the boron concentration in the films). In all cases the substrate temperature was 850 °C. The first point to the left corresponds to the non-intentionally-doped sample. As can be seen, the conductivity for this nominally intrinsic sample is around $8 \times 10^{-6}\,\Omega^{-1}$ cm^{-1}. The addition of a small amount of boron leads to a decrease of the conductivity, which reaches a minimum value of $\sim 2 \times 10^{-7}\,\Omega^{-1}$ cm^{-1}. This is evidence that the nominally intrinsic samples are slightly of the *n*-type. Other groups have also reported that films produced with no intentionally added dopants resulted in *n*-type [2,18,27,28]. The conductivity of the compensated sample, $\sim 2 \times 10^{-7}\,\Omega^{-1}$ cm^{-1}, is even lower than that of intrinsic crystalline silicon (around $4 \times 10^{-6}\,\Omega^{-1}$ cm^{-1}). This is probably due to a decrease of the carriers' mobility compared to that of intrinsic crystalline silicon, since transport should take place across grain boundaries in the coplanar geometry used for the conductivity measurements. A further increase in the boron content leads to *p*-doped samples, with gradually increasing conductivities (Fig. 9). For one of these *p*-doped samples, having a dark conductivity of 0.15 Ω^{-1} cm^{-1}, we have performed Hall effect measurements. We obtained a hole concentration of 5×10^{17} cm^{-3} and a Hall hole mobility of 1.9 cm^2 V^{-1} s^{-1}, a reasonable value for a *p*-doped sample of sub-micrometer grain size without any hydrogen passivation of intergrain defects and impurities. For an even higher doping concentration we obtained a conductivity as high as 8 Ω^{-1} cm^{-1}. According to the comparison made in [16], the concentration of acceptors that gives a conductivity of 8 Ω^{-1} cm^{-1} in poly-Si is $\sim 10^{18}$ cm^{-3}. Therefore, we are in the range of carrier concentrations needed for the absorber layer of a solar cell.

Figure 9 also presents (squares, left scale) the variation of the dark conductivity activation energy with the BBr_3 temperature. The behavior of the activation energy is consistent with that of the room-temperature dark conductivity, with values around 0.5 eV for the undoped sample, an increase to $\sim$0.61 eV for the compensated sample and a decrease to $\sim$0.009 eV for the heavily doped samples. The value for the compensated sample, 0.61 eV, is higher than half the bandgap of crystalline silicon (0.56 eV). This is probably due to a statistical shift of the Fermi energy during the measurement, or to a conductivity dominated by electrons – because of their much higher mobility – even when the Fermi energy is closer to the valence band tail.

In summary, a range of doping conditions – slightly *n*-type, compensated and clearly *p*-type – can be obtained. The viability of doping opens the possibility to deposit *p*-*n* or *p*-*i*-*n* solar cell structures. However, a further increase in doping concentration would be needed to obtain the heavily *p*-doped layers that constitute the back surface field of a solar cell.

4 Conclusions

In this work, we present results of the deposition of thin polycrystalline silicon films on glass substrates at intermediate temperatures. The precursor gas (TCS) and the substrate (aluminosilicate glass), both of low cost, proved to be adequate for silicon deposition, since the chemical reaction took place at temperatures much lower than the glass softening point. The films were homogeneous and well adhered to the substrate, and exhibited a columnar structure suitable for the electrical conduction in a photovoltaic cell. Moreover, a strong (2 2 0) preferential orientation is indicative of a low density of intra-grain defects, being also a favorable characteristic.

Under the deposition conditions that we used, deposition rates compatible with industrial applications were obtained. Although the grain size is lower than 0.4 μm, this should not be an obstacle to obtaining good photovoltaic properties. Moreover, a naturally textured surface would provide an increased light trapping. The dark conductivity activation energy showed that the non-intentionally doped films are intrinsic, proving that the films do not contain electrically active defects or impurities. On the other hand, the possibility of boron doping has been shown. In conclusion, our results demonstrate the feasibility of directly depositing polycrystalline silicon thin-film solar cells on glass substrates by AP-CVD at intermediate temperatures.

This work was supported by ANPCyT (Projects 22-32515 and 22-25749), CONICET (Project PIP 1464) and UNL (Project CAI+D 68-349).

References

1. G. Beaucarne, S. Bourdais, A. Slaoui, J. Poortmans, Thin Solid Films **403**, 229 (2002)
2. G. Beaucarne, S. Bourdais, A. Slaoui, J. Poortmans, Appl. Phys. A **79**, 469 (2004)
3. A. Eyer, F. Haas, T. Kieliba, D. Osswald, S. Reber, W. Zimmermann, W. Warta, J. Cryst. Growth **225**, 340 (2001)
4. K.M. Sarma, M.J. Rice, J. Cryst. Growth **56**, 313 (1982)
5. A. Focsa, I. Gordon, G. Beaucarne, O. Tuzun, A. Slaoui, J. Poortmans, Thin Solid Films **516**, 6896 (2008)
6. R. Ludemann, S. Schaefer, C. Schule, C. Hebling, in *Proc. of 26th IEEE Photovoltaic Specialists Conf., Anaheim, CA, USA, 1997*, p. 159
7. R.B. Bergmann, J.G. Darrant, A.R. Hyde, J.H. Werner, J. Non-Cryst. Solids **218**, 388 (1997)
8. R. Brendel, R.B. Bergmann, P. Lölgen, M. Wolf, J.H. Werner, Appl. Phys. Lett. **70**, 390 (1997)
9. L.R. Pinckney, J. Non-Cryst. Solids **255**, 171 (1999)
10. I. Gordon, L. Carnel, C. Van Gestel, G. Beaucarne, J. Poortmans, L. Pinckney, A. Mayolet, in *Proc. of 22nd European Photovoltaic Solar Energy Conf., Milan, Italy, 2007*, p. 1993
11. R.B. Bergmann, R. Brendel, M. Wolf, P. Lölgen, J. Krinke, H.P. Strunk, J. Werner, Semicond. Sci. Technol. **12**, 224 (1997)
12. R. Brendel, R.B. Bergmann, B. Fischer, J. Krinke, R. Plieninger, U. Rau, J. Reiß, H.P. Strunk, H. Wanka, J.H. Werner, *Proceedings 26th IEEE Photovoltaic Specialists Conf., Anaheim, CA, USA, 1997*, p. 635
13. I. Gordon, D. Van Gestel, Y. Qiu, S. Venkatachalam, G. Beaucarne, J. Poortmans, *Proc. of 23rd European Photovoltaic Solar Energy Conf., Valencia, Spain, 2008*, p. 2053
14. I. Gordon, S. Vallon, A. Mayolet, G. Beaucarne, J. Poortmans, Sol. Energy Mater. Sol. Cells **94**, 381 (2010)
15. Datasheet of glass AF37, SCHOTT Displayglass Jena GmbH (2004)
16. S. Bourdais, G. Beaucarne, J. Poortmans, A. Slaoui, Physica B **273**, 544 (1999)
17. L. Carnel, I. Gordon, D. Van Gestel, G. Beaucarne, J. Poortmans, A. Stesmans, J. Appl. Phys. **100**, 063702 (2006)
18. D. Angermeier, R. Monna, A. Slaoui, J.C. Muller, J. Cryst. Growth **191**, 386 (1998)
19. A. Slaoui, R. Monna, D. Angermeier, S. Bourdais, J.C. Muller, in *Proc. of 26th IEEE Photovoltaic Specialists Conf., Anaheim, CA, USA, 1997*, p. 627
20. G. Harbeke, L. Jastrzebski, J. Electrochem. Soc. **137**, 696 (1990)
21. G.W. Cullen, M.S. Abrahams, J.F. Corboy, M.T. Duffy, W.E. Ham, L. Jastrzebski, R.T. Smith, M. Blumenfeld, G. Harbeke, J. Lagowski, J. Cryst. Growth **56**, 281 (1982)
22. G. Beaucarne, J. Poortmans, M. Caymax, J. Nijs, R. Mertens, SSP **67**, 577 (1999)
23. A. Focsa, I. Gordon, J.M. Auger, A. Slaoui, G. Beaucarne, J. Poortmans, C. Maurice, Renew. Energy **33**, 267 (2008)
24. D. Angermeier, R. Monna, S. Bourdais, A. Slaoui, J.C. Muller, Prog. Photovolt. Res. Appl. **6**, 219 (1998)
25. Y. Ishikawa, Y. Yamamoto, T. Hatayama, Y. Uraoka, T. Fuyuki, Sol. Energy Mater. Sol. Cells **74**, 255 (2002)
26. J.H. Werner, R. Dassow, T.J. Rinke, J.R. Kohler, R.B. Bergmann, Thin Solid Films **383**, 95 (2001)
27. G. Beaucarne, I. Gordon, D. Van Gestel, L. Carnel, J. Poortmans, *Proc. of 21st European Photovoltaic Solar Energy Conf., Dresden, Germany, 2006*, p. 721
28. B. Rau, I. Sieber, B. Selle, S. Brehme, U. Knipper, S. Gall, W. Fuhs, Thin Solid Films **451–452**, 644 (2004)